Supporting Information

Copper(I) halide polymers derived from tris[2-(pyridin-2-yl)ethyl]phosphine: halogen-tunable colorful luminescence spanning from deep blue to green

Alexander V. Artem'ev,*[a] Andrey Yu. Baranov,[a] Mariana I. Rakhmanova,[a] Svetlana F. Malysheva,[b] Denis G. Samsonenko[a]

[a] *Nikolaev Institute of Inorganic Chemistry, 3, Acad. Lavrentiev Ave., Novosibirsk 630090, Russian Federation*
[b] *A. E. Favorsky Irkutsk Institute of Chemistry, Siberian Branch of Russian Academy of Sciences, Russian Federation*

*Author for correspondence: chemisufarm@yandex.ru (Alexander V. Artem'ev)

Table of Contents

§1. X-Ray crystallography

Single crystals of **3**·0.5CH_3CN were grown by vapor diffusion of diethyl ether into an acetonitrile solution at room temperature. Diffraction data were obtained on an automated Agilent Xcalibur diffractometer equipped with an area AtlasS2 detector (graphite monochromator, λ(MoKα) = 0.71073 Å, ω-scans). Integration, absorption correction, and determination of unit cell parameters were performed using the CrysAlisPro program package.[1] The structures were solved by dual space algorithm (SHELXT[2]) and refined by the full-matrix least squares technique (SHELXL[3]) in the anisotropic approximation (except hydrogen atoms). Positions of hydrogen atoms were calculated geometrically and refined in the riding model.

The crystallographic data and details of the structure refinements are summarized in Table S1. CCDC 1982609 contains the supplementary crystallographic data for this paper. These data can be obtained free of charge from The Cambridge Crystallographic Data Center at http://www.ccdc.cam.ac.uk/data_request/cif.

Table S1. Crystal data and structure refinement for **3**·0.5CH_3CN.

CCDC number	1982609
Chemical formula	$C_{22}H_{25.5}Cu_2I_2N_{3.5}P$
M_r	750.81
Crystal system, space group	Triclinic, $P^{\bar{}}1$
Temperature (K)	130
a, *b*, *c* (Å)	9.4902(3), 12.2629(5), 12.5114(5)
α, *β*, *γ* (°)	113.970(4), 102.843(3), 97.774(3)
V (Å^3)	1254.92(9)
Z	2
μ (mm^{-1})	4.23
Crystal size (mm)	0.25 × 0.10 × 0.04
T_{min}, T_{max}	0.748, 1.000
No. of measured, independent and observed [$I > 2\sigma(I)$] reflections	12408, 6409, 5532
R_{int}	0.023
$(\sin \theta/\lambda)_{max}$ (Å^{-1})	0.711
$R[F^2 > 2s(F^2)]$, $wR(F^2)$, S	0.025, 0.053, 1.01
No. of reflections	6409
No. of parameters	290
$\Delta\rangle_{max}$, $\Delta\rangle_{min}$ (e Å^{-3})	0.65, –0.58

[1] CrysAlisPro 1.171.38.46, *Rigaku Oxford Diffraction*, 2015.
[2] G. M. Sheldrick *Acta Crystallogr.*, **2015**, *A71*, 3–8.
[3] G. M. Sheldrick, *Acta Crystallogr.*, **2015**, *C71*, 3–8.

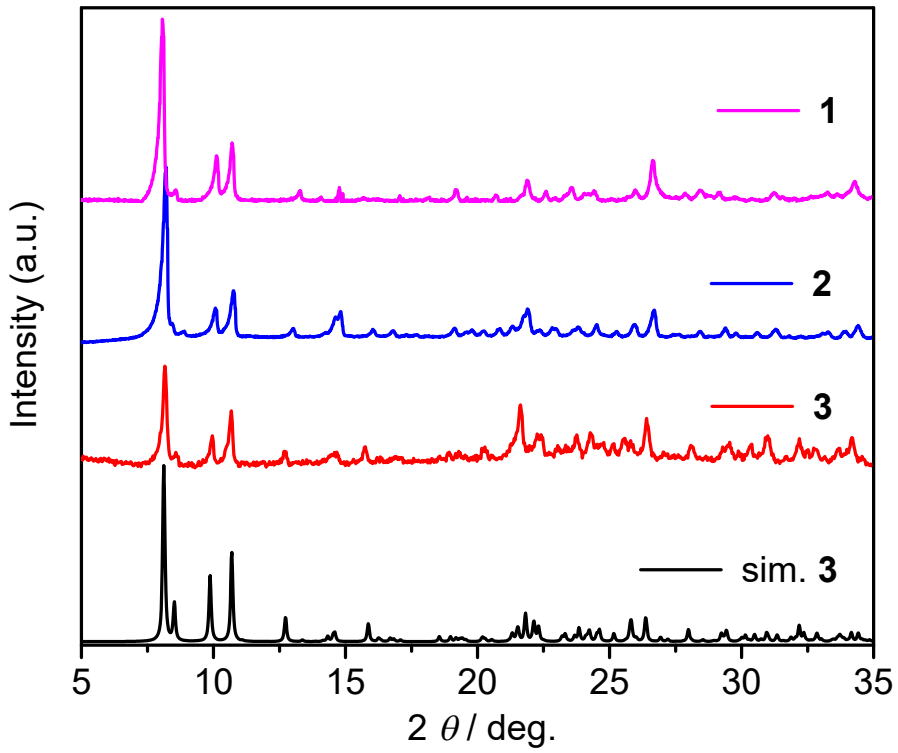

Figure S1. Experimental XRPD patterns for **1**–**3** compared with the simulated one for **3**·0.5CH_3CN.

§2. FT-IR spectra

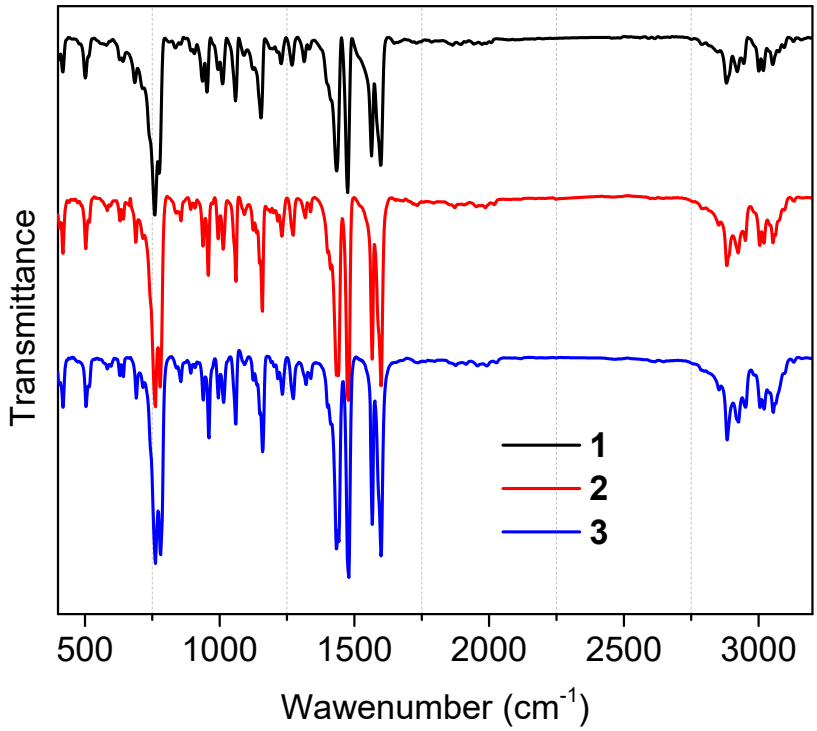

Figure S2. FT-IR spectra of **1**–**3** showed in the 400–3200 cm^{-1} region.

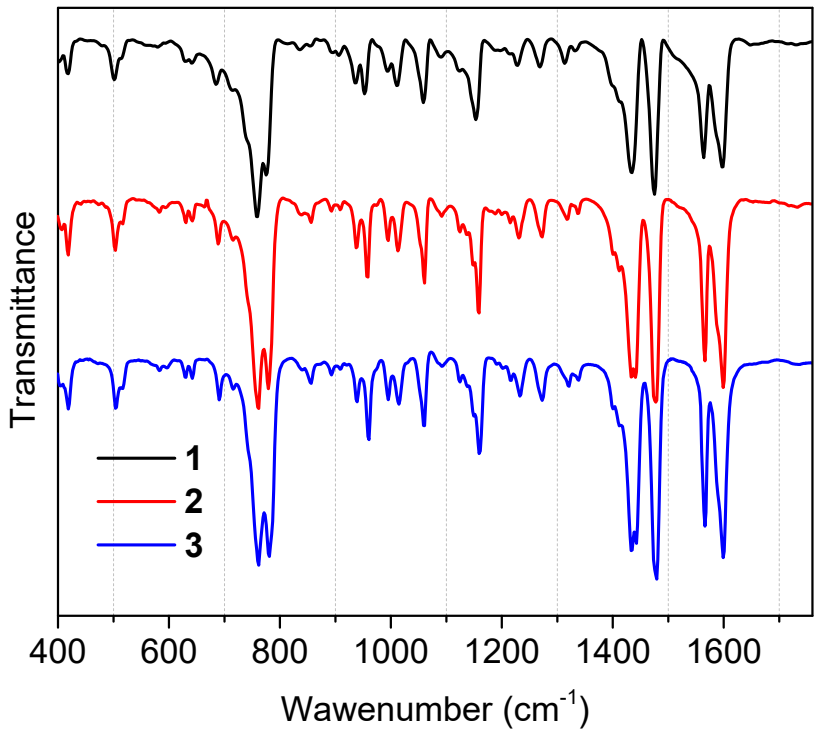

Figure S3. FT-IR spectra of **1**–**3** showed in the fingerprint region.

§3. Computational details

Figure S4. Five lowest unoccupied and 12 highest occupied MOs (iso-value = 0.04) for the S_0 state of the model $\{Cu_4I_4L_2\}$ fragment of CP **3** calculated at the B3LYP/LANL2DZ/6-31+G(d,p) level.

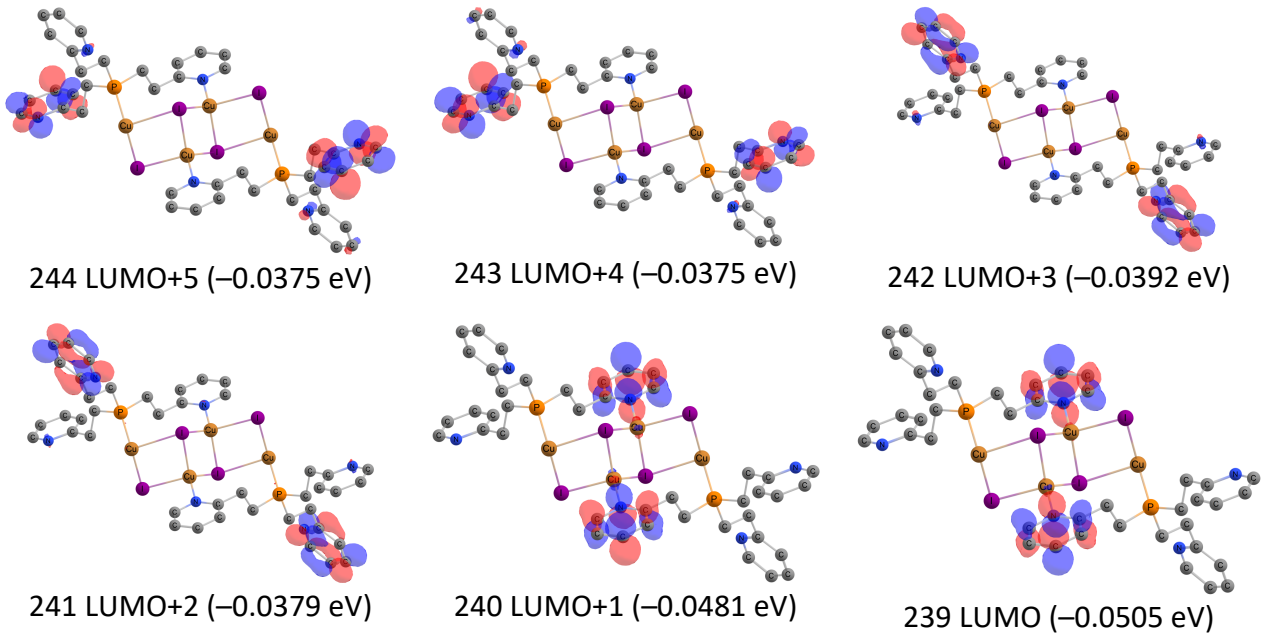

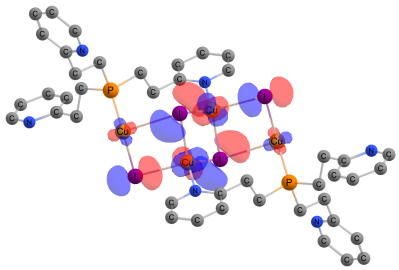

HOMO (–0.1822 eV)

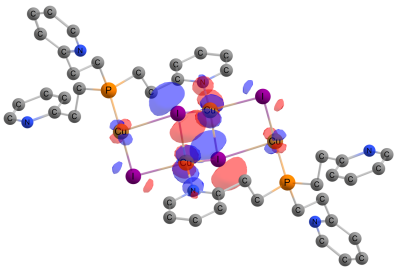

HOMO–1 (–0.1845 eV)

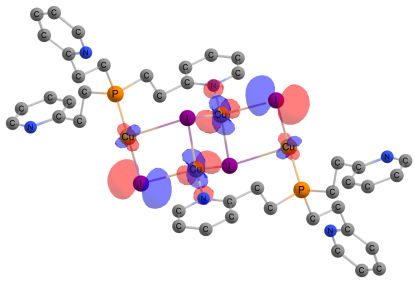

HOMO–2 (–0.1956 eV)

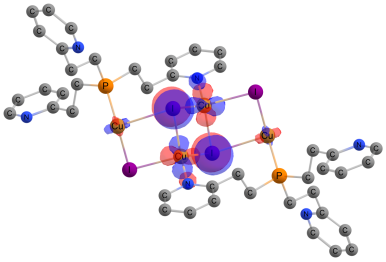

HOMO–3 (–0.1967 eV)

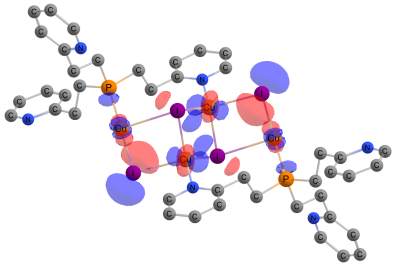

HOMO–4 (–0.1986 eV)

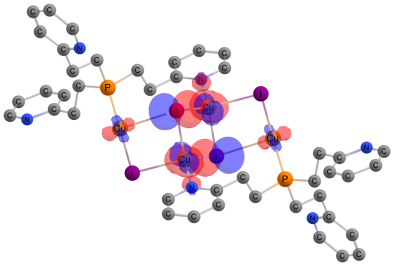

HOMO–5 (–0.2030 eV)

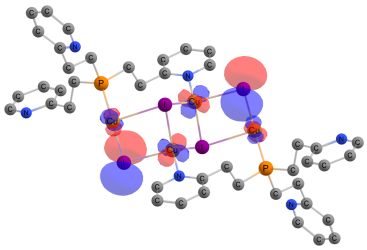

HOMO–6 (–0.2068 eV)

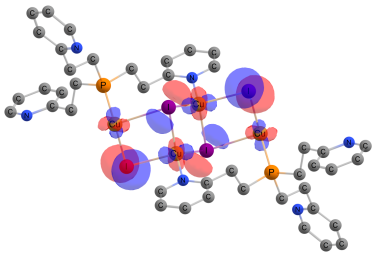

HOMO–7 (–0.2096 eV)

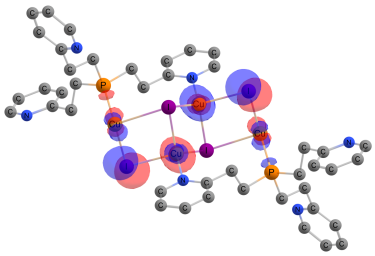

HOMO–8 (–0.2199 eV)

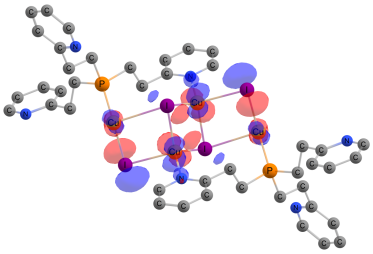

HOMO–9 (–0.2239 eV)

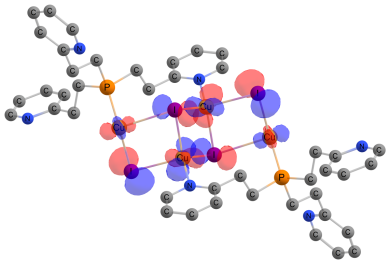

HOMO–10 (–0.2316 eV)

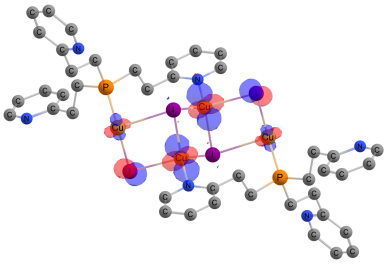

HOMO–11 (–0.2333 eV)

Table S2. The main singlet-singlet electronic transitions (f > 0.004) in the absorption spectrum of **3** derived from TD-DFT calculations of the model $\{Cu_4I_4L_2\}$ fragment at B3LYP/LANL2DZ/6-31+G(d,p) level (S_0 state, gas).

E, eV	λ, nm	f [(a)]	Transitions (main contributions)	Character [(b)]
2.94	421.0	0.0159	HOMO–1 → LUMO (19.8%) HOMO → LUMO (75.7%)	(M+X)LCT
2.98	415.6	0.0108	HOMO–1 → LUMO (68.7%) HOMO → LUMO (20.6%)	(M+X)LCT
3.27	379.0	0.0080	HOMO–1 → LUMO (59.4%) HOMO–2 → LUMO (20.8%)	(M+X)LCT
3.32	373.7	0.0420	HOMO → LUMO+2 (36.2%) HOMO → LUMO+7 (25.8%)	(M+X)LCT + (M+I)MCT

3.38	366.5	0.0239	HOMO–1 → LUMO (11.7%) HOMO–1 → LUMO+2 (33.3%) HOMO–1 → LUMO+7 (22.4%) HOMO → LUMO+2 (14.7%)	(M+X)LCT + (M+I)MCT
3.44	360.5	0.0093	HOMO–3 → LUMO (16.9%) HOMO–2 → LUMO+1 (56.4%)	(M+X)LCT
3.48	356.3	0.0080	HOMO–6 → LUMO (14.5%) HOMO–4 → LUMO+1 (74.7%)	(M+X)LCT
3.57	346.8	0.0133	HOMO–5 → LUMO+1 (74.8%)	(M+X)LCT
3.65	339.9	0.0089	HOMO–6 → LUMO (23.5%) HOMO–1 → LUMO+2 (14.2%) HOMO → LUMO+9 (16.2%)	(M+X)LCT
3.72	333.2	0.0449	HOMO–3 → LUMO+2 (38.0%) HOMO–3 → LUMO+7 (24.7%)	(M+X)LCT + (M+I)MCT
3.78	328.2	0.0146	HOMO–6 → LUMO (15.3%) HOMO–2 → LUMO+3 (16.8%) HOMO–2 → LUMO+6 (14.1%)	(M+X)LCT + (M+I)MCT
3.84	322.8	0.0042	HOMO–7 → LUMO+1 (71.6%)	(M+X)LCT
4.00	309.6	0.0053	HOMO–3 → LUMO+5 (67.0%)	(M+X)LCT
4.02	308.6	0.0081	HOMO–1 → LUMO+11 (21.9%) HOMO → LUMO+12 (48.8%)	(M+X)LCT
4.03	307.6	0.0046	HOMO–4 → LUMO+4 (51.7%)	(M+X)LCT
4.05	306.3	0.0053	HOMO–4 → LUMO+3 (24.8%) HOMO–4 → LUMO+4 (23.5%) HOMO–4 → LUMO+6 (30.0%)	(M+X)LCT
4.05	305.9	0.0192	HOMO–6 → LUMO+7 (19.5%) HOMO–4 → LUMO+3 (16.2%)	(M+X)LCT + (M+I)MCT
4.07	304.5	0.0047	HOMO–1 → LUMO+12 (87.5%)	(M+X)LCT

[(a)] Oscillator strength;

[(b)] (M+X)LCT and (M+I)MCT denoted to the transitions of (copper+iodine)-to-ligand charge transfer and (copper+iodine)-to-copper charge transfer nature, respectively.

§4. Photophysical measurements

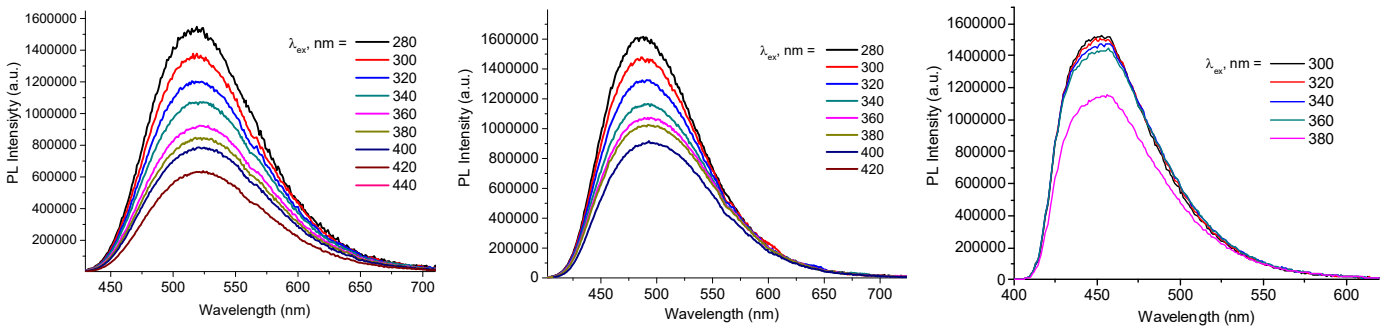

Figure S5. The emission spectra of **1**–**3** recorded at different excitations (300 K).

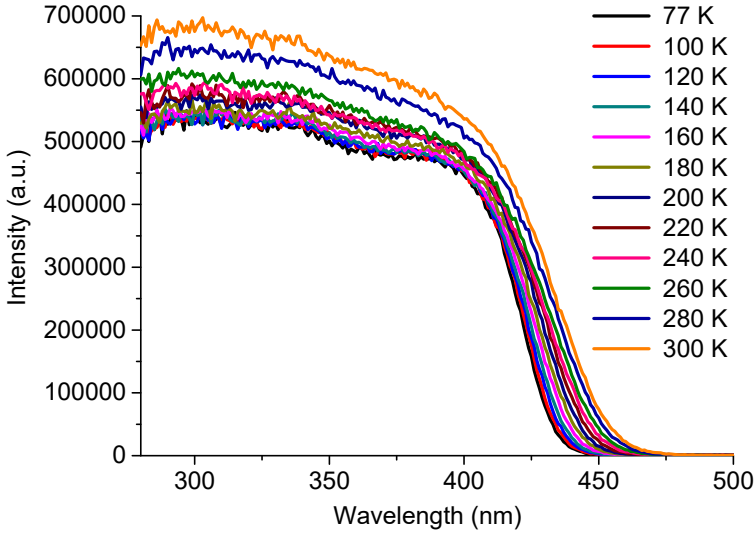

Figure S6. Temperature-dependent excitation spectra of **1** (λ_{em} = 520 nm).

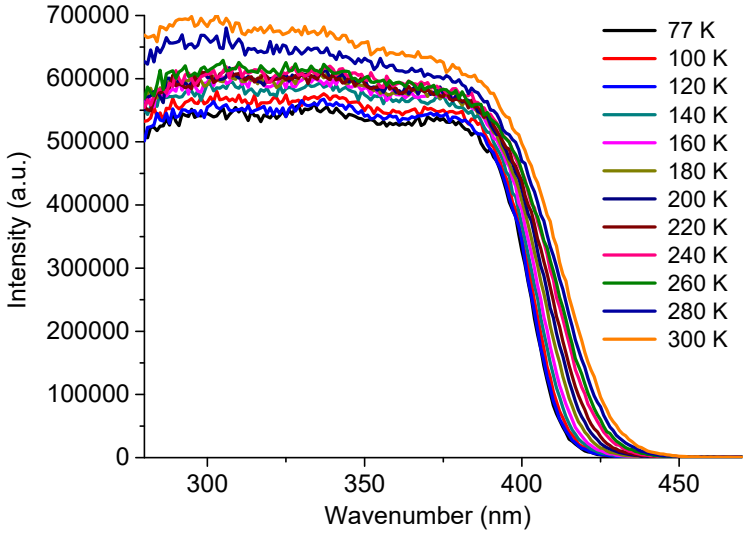

Figure S7. Temperature-dependent excitation spectra of **2** (λ_{em} = 490 nm).

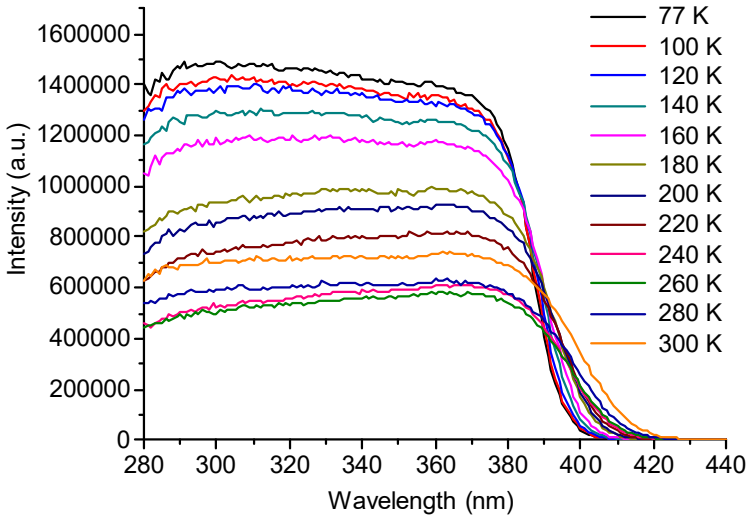

Figure S8. Temperature-dependent excitation spectra of **3** (λ_{em} = 450 nm).